Proceedings of the Seventeenth International Conference on
Civil, Structural and Environmental Engineering Computing
Edited by: P. Iványi, J. Kruis and B.H.V. Topping
Civil-Comp Conferences, Volume 6, Paper 6.3
Civil-Comp Press, Edinburgh, United Kingdom, 2023
doi: 10.4203/ccc.6.6.3

Numerical assessment of lateral capacity of concrete Maya vaults at Bonampak, Chiapas, México

A. Remus[1], H. Kimanya[1], S. Tezcan[1,2] and R. Perucchio[1]

[1]Department of Mechanical Engineering, University of Rochester, NY, United States of America
[2]Department of Mechanics, Bilecik Şeyh Edebali University, Bilecik, Turkey

Abstract

Concrete vaults of the Late Classic Maya complex of Bonampak, Chiapas, Mexico (580-800 C.E.) are well-preserved examples of the one-story, corbelled style of the Maya and they house some of the best examples of murals in the Americas. To assess the monuments in light of the seismic risk of the region and the structures' cultural value, the present work compares sectional finite element (FE) models of Structures 1 and 3 to the lateral capacities produced using kinematic limit analysis (KLA). A sensitivity analysis of the model's tensile strength shows that as material strength approaches zero, FE analyses converge to the lateral capacities defined using KLA. Modelling is performed in Abaqus/CAE Explicit, which allows for large deformations without numerical failure. The concrete damaged plasticity (CDP) formulation is adopted for Maya concrete. This paper illustrates that the results of KLA are conservative estimates for lateral capacity and that the presence of non-zero tensile strength may significantly increase lateral capacity. Further 3D analysis reinforces the validity of these claims and the FE approach.

Keywords: Maya vaults, Maya concrete, dynamic analysis, nonlinear finite element analysis, concrete damaged plasticity, lateral capacity

1 Introduction

The exemplary Maya vaults at the Bonampak complex in Chiapas, México are well-preserved despite their position in a seismically active region [1]. Since the 1940s, researchers have studied the site's architecture, art motifs, and hieroglyphics, and they have determined that it is one of several cities in a culturally uniform Maya region. The influence of Yaxchilán, 20 km north of Bonampak has been identified as the politically-dominating power during its existence from 580-800 C.E. [2].

Figure 1 Bonampak and Yaxchilan in Chiapas, Mexico, near Guatemala. Regional seismic hazard is high (right) [1].

One of the most famous aspects of the archaeological complex is the presence of fine murals protected within each vaulted structure (

Figure 2), and this motivates structural assessment in multiple buildings at the site. The historical, archaeological, and cultural value of these in situ works of art is unmatched by other Maya murals in the Americas.

Figure 2 Structures at Bonampak are situated on stepped man-made terraces. The interior of Structure 1 (right) contains several murals, including the one pictured.

The architectural pattern of these one-story structures is that of a thick corbelled vault supported by mortared limestone walls. Lime-based concrete fills the space between the small limestones that line the extrados and larger limestones used to face the intrados. They are constructed on artificial earthen terraces, some of which have settled unevenly and rotated the supporting foundation of the structures (

Figure 3).

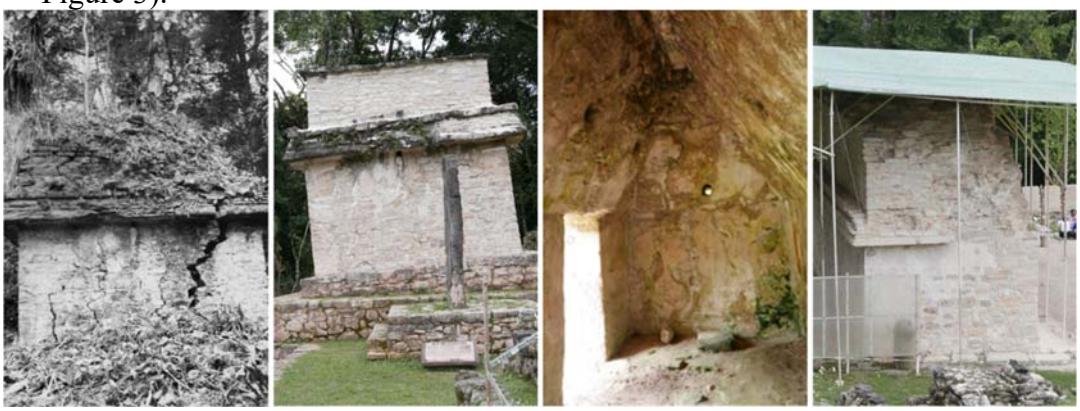

Figure 3 From left to right: 1955 damage [3], base rotation of Structure 3, interior of Structure 3, exterior damage to Structure 1.

The present settlement and potential for further settlement, together with the high seismic risk of the region [1], compels refined analysis of structures at the site [1]. Structures 1 and 3 in particular have been investigated because they house the better-preserved murals of the site [4,5]. The authors presently undertake a careful re-assessment of earlier kinematic limit analysis by Flores Espino and Orea Magaña [4] with an analogous, nonlinear, finite element (FE) model of the same 3D section. Using Abaqus/CAE Explicit [6], we performed a sensitivity analysis that gradually decreased the material strength of Maya concrete, approaching the zero-strength assumption inherent to KLA. Maya concrete was modelled with the concrete damaged plasticity (CDP) formulation. The results are discussed in light of the peak ground acceleration (PGA) demand for the region, 0.255g [1].

2 Model and Simulation

2.1 Geometry

Measurements for the models of Structures 1 and 3 reflect surveys by Ruppert and his colleagues [2] and match the section geometry defined by Flores and Orea [4]. Idealizations that ensure numerical stability of the mesh are illustrated in Figure 4; namely, the flattening of non-structural detail on the borders above doorways and the removal of the remains of Structure 3's rooftop *crestería* or "roof comb" (visible in Figure 2).

A *crestería*, or "roof comb," is common in Maya architecture [7]. Though there is evidence of this ornamental feature on Structure 3 and others at the site, the model was constructed based on the extant state of Structure 3, in which the crestería has collapsed. Reconstruction to a supposed original state aligns with that of previous work [2,4]. The sectional models shown are half of the symmetric models published

in [4]. They are implemented in Abaqus/CAE Explicit with a symmetry plane as shown in Figure 6 to reduce the computational cost of the analysis.

2.2 Material

The material properties for Maya concrete have been studied at various Maya sites. We have implemented the concrete damaged plasticity (CDP) formulation for quasi-brittle materials [6,8] following previous FE modelling of the site's vaults where the derivation has been discussed in more detail [5,9].

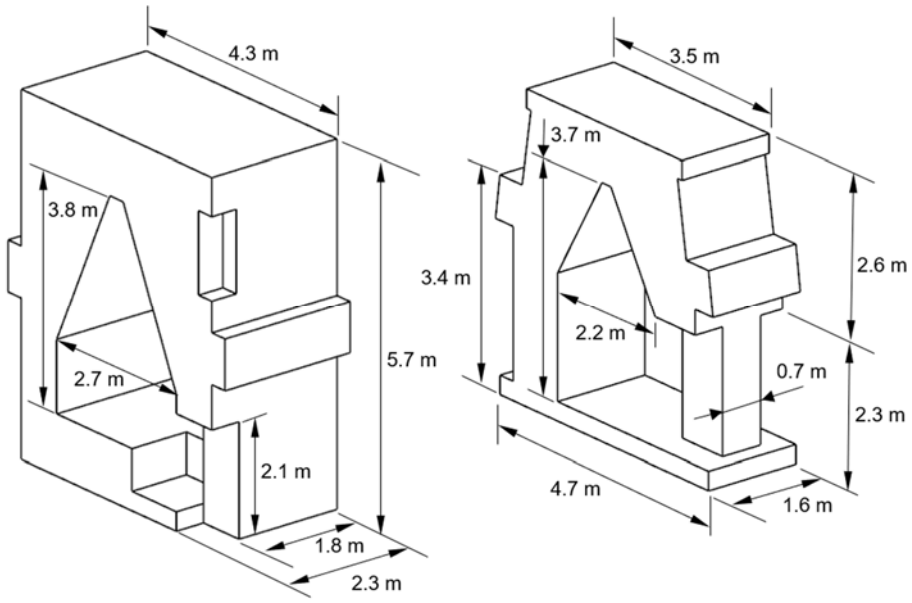

Figure 4 Section geometry for Structures 1 (left) and 3 (right) is idealized from [2,4].

Young's Modulus [GPa]	Density [kg·m^{-3}]	Poisson's Ratio [/]	Compressive Strength [MPa]	Tensile Strength [MPa]
3.69	1,873	0.2	6.25	0.625

Table 1 Elastic behaviour parameters for CDP implementation of Maya concrete.

Table 1 lists the parameters necessary for the elastic range of behaviour, and parameters for plastic behaviour are shown in

Table 2. Curves showing the nonlinear behaviour representing Maya concrete are reproduced in

Figure 5, which illustrates a tensile strength that is one-tenth of the compressive behaviour of Maya concrete.

Dilation Angle	Eccentricity	F_{b0}/f_{c0}	K	Viscosity Parameter

[deg]	[/]	[/]	[/]	[/]
31	0.1	1.16	0.67	0.0001

Table 2 Plastic behaviour parameters required for CDP implementation of Maya concrete in Abaqus.

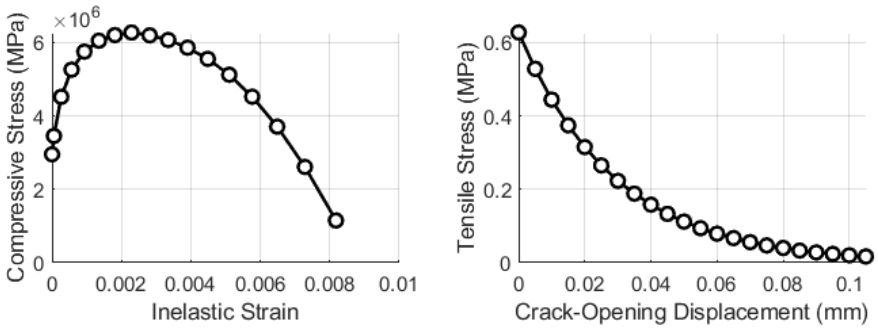

Figure 5 Definition of postcritical behavior in compression (left) and tension (right).

The one-tenth assumption for quasi-brittle material is a common standard for masonry tensile strength [10]. The present work scales the postcritical behaviour to test the sensitivity of lateral capacity to tensile strength. Approaching nil tensile strength allows us to compare our results with those of KLA. Tensile behaviours are defined by fractions of compressive strength: 1/10, 1/30, 1/50, 1/100, and 1/150. Going forward, the tensile behaviour defined by 1/10 of compressive strength will be referred to as F10, and so on: F30, F50, F100, F150.

2.3 Boundary Conditions, Loading, and Mesh

The investigated structures are modelled as idealized 2D sections. Each model uses symmetry planes (1 and 2 in Figure 6) to produce a "quasi-plane strain" condition and to simulate the presence of an infinite continuation of the structure beyond the section. A proposed "quasi-plane stress" condition that omits plane 2 is investigated with the Structure 1 section.

The models do not include the man-made terraces upon which they are built; instead, the structures are fully encastred at the base (plane 3 in Figure 6). The gravity load is applied as linear ramp over 5 seconds for all simulations in order to enforce quasi-static conditions during the analysis.

Two methods of application of lateral acceleration are compared using Structure 1. In the first case, acceleration is applied directly to the structure as a uniform body force. The load linearly increases with time and is applied in the anticipated direction of collapse, producing a pushover condition. The second, more realistic method, accelerates the base (plane 3) to incite inertial forces as the cause of collapse. This method is implemented for simulations of Structure 3 as well. In this latter case, the encastred condition in plane 3 is modified during the lateral acceleration step to allow

motion in the x-direction. Acceleration is applied opposite to the anticipated collapse direction to produce the correct inertial response. Both methods apply a load of 0.75g over 7.5 seconds, a rate of 0.1g/sec.

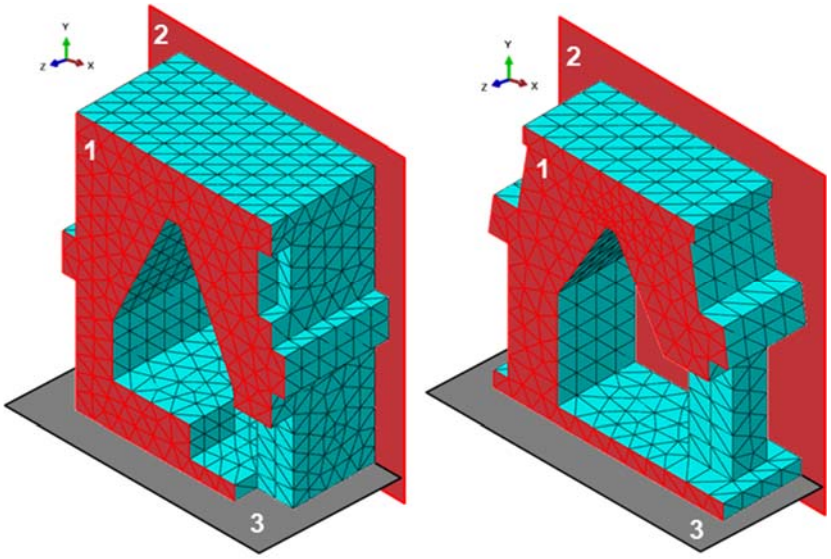

Figure 6 Mesh and boundary planes for Structures 1 (left) and 3 (right). Quasi-plane stress models exclude plane 2 boundaries.

2.4 Determination of failure

We analyse energy outputs from Abaqus/CAE to quantitatively determine a point of collapse that can be compared between models. The point at which some portion(s) of a structure begin to collapse is accompanied by separation of the structure into parts that then enter a dynamic state. Kinetic energy (KE) from this phenomenon grows asymptotically at the point of failure and is a clear indicator of collapse for models that apply lateral acceleration to the entire body.

As shown in
Figure 7 (dark red), KE grows asymptotically at the same point as plastic dissipation energy (PD). This can be explained by the implementation of the CDP formulation, which relies on an analogy between plastic strains and fracture. The separation of the structure that leads to asymptotic KE is precipitated by the propagation of a fracture. Due to the relationship between plastic strains and fracture in the CDP formulation, fracture propagation is accompanied by PD.

For analyses that implement basal acceleration to incite inertial collapse, kinetic energy due to collapse cannot be extracted from total kinetic energy produced by applying the lateral load. However, the PD asymptote is present. Its intersection with elastic strain energy (SE) is used to define failure and corresponds to the point at which the structure must dissipate more energy than it can store.

3 Results

Analyses using the Structure 1 section were performed in order to compare the effects of body versus base acceleration and the quasi-plane stress versus quasi-plane strain boundary conditions. Each comparison was made with each of the five tensile strengths discussed in the subsection "Material" of the preceding section.

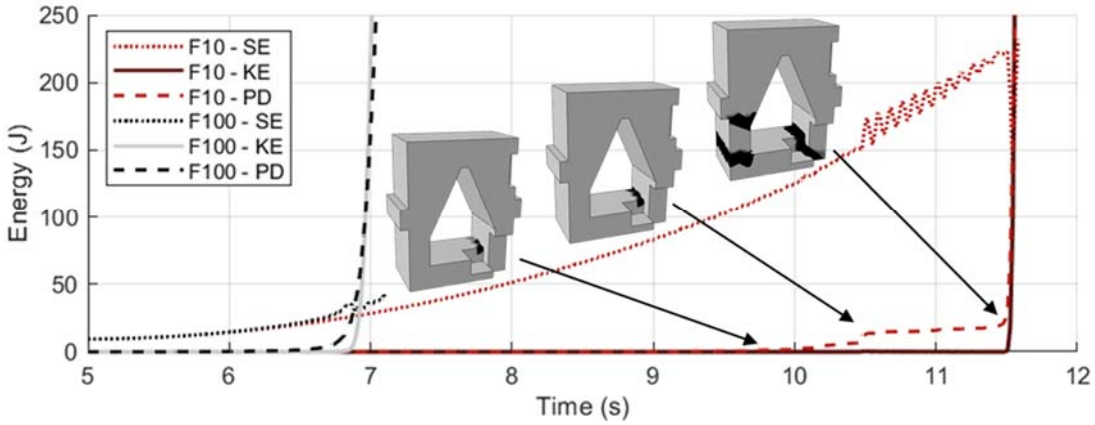

Figure 7 Elastic strain (SE), kinetic (KE) and plastic dissipation (PD) energies from the F10 and F100 models of Structure 1. Insets reflect quasi-plane strain, F10 (red).

Figure 7 gives a sample of results from body acceleration that illustrate the consistency of asymptotes for PD and KE. The inset images illustrate how the development of fractures in the monument can be linked to changes in PD: the propagation of dark grey and black zones of the model correspond to areas of fracture at the time instants of the indicated increases in PD.

Next, a comparison of boundary conditions was made (Figure 8). Removing the symmetry condition of plane 2 (Figure 6) to produce a quasi-plane strain condition is shown to produce results that are nearly identical to the quasi-plane strain condition of symmetry on planes 1 and 2.

We assume that the quasi-plane strain condition more accurately represents the continuity of the structure in 3D and maintained this condition for subsequent analyses. For each tensile strength, two analyses under quasi-plane strain were performed: one with basal acceleration and one with body acceleration. Failure instants for each model were determined using energy outputs as described above in the section "2.4 Determination of **failure**," and they are compared in

Figure 7. The damage patterns at failure for basal acceleration simulations are reproduced in

Figure 10.

The analysis of Structure 3 selects quasi-plane strain boundary conditions and basal acceleration as the most realistic simulation possible for a section: the plane strain condition implies a continuation of the structure beyond the model and basal acceleration most closely mimics the acceleration of the ground during a seismic event. The simulations evaluate a non-inclined configuration and 6-degree inclination configuration that reflects the monument's present state. The results for both are compiled in Figure 11.

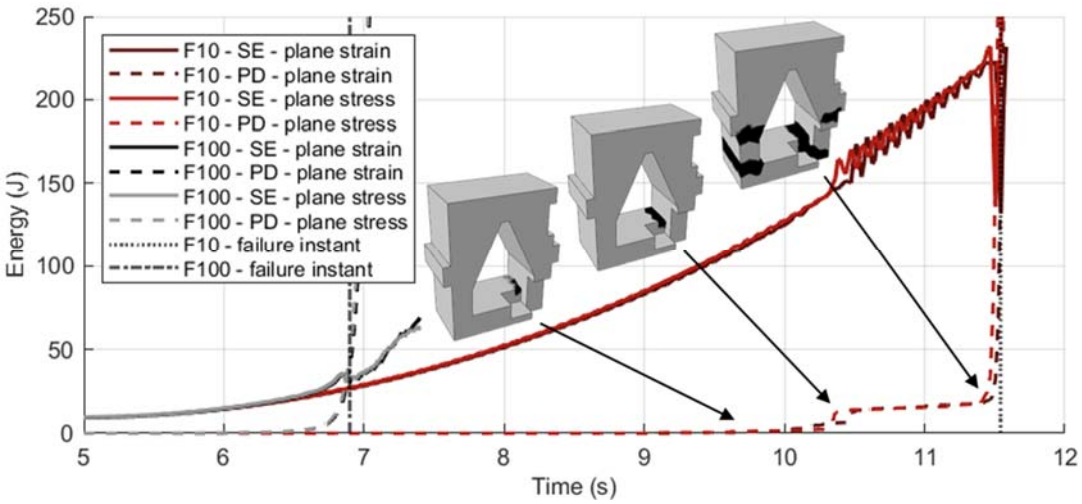

Figure 8 Comparison of SE and PD results from quasi-plane strain and quasi-plane stress models of Structure 1. Note that F100 results are nearly superimposed. Insets reflect quasi-plane stress, F10 (bright red).

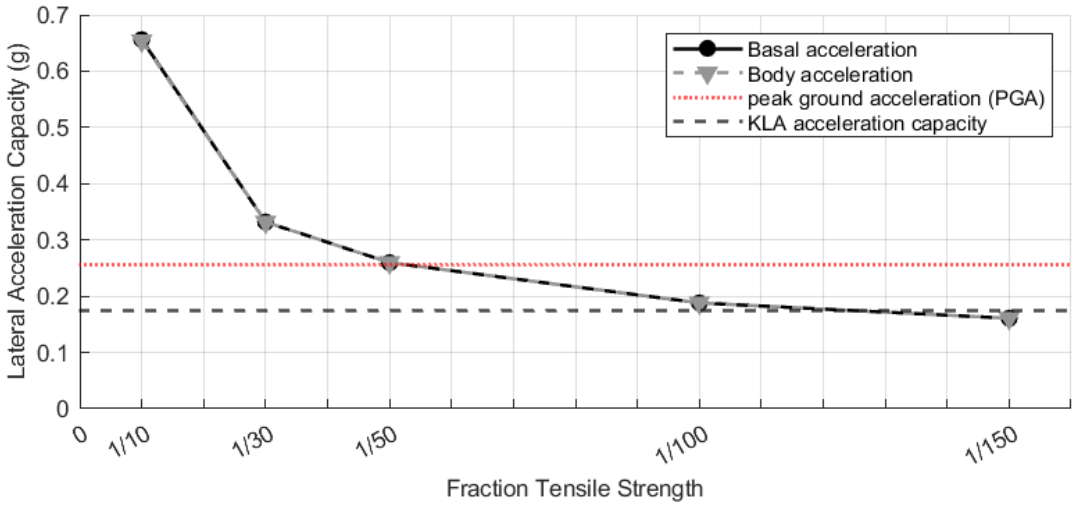

Figure 9 Structure 1 sections produce lateral capacity values that converge to the capacity determined from KLA as tensile strength decreases.

Both

Figure 9 and Figure 11 show that decreasing the material tensile strength produces results that converge towards the lateral capacity determined using kinematic limit analysis (KLA), noted with segmented horizontal lines [4]. Structure 1 converges to nearly the same value, while the inclined and non-inclined version of Structure 3 converge to a value about 0.1g higher.

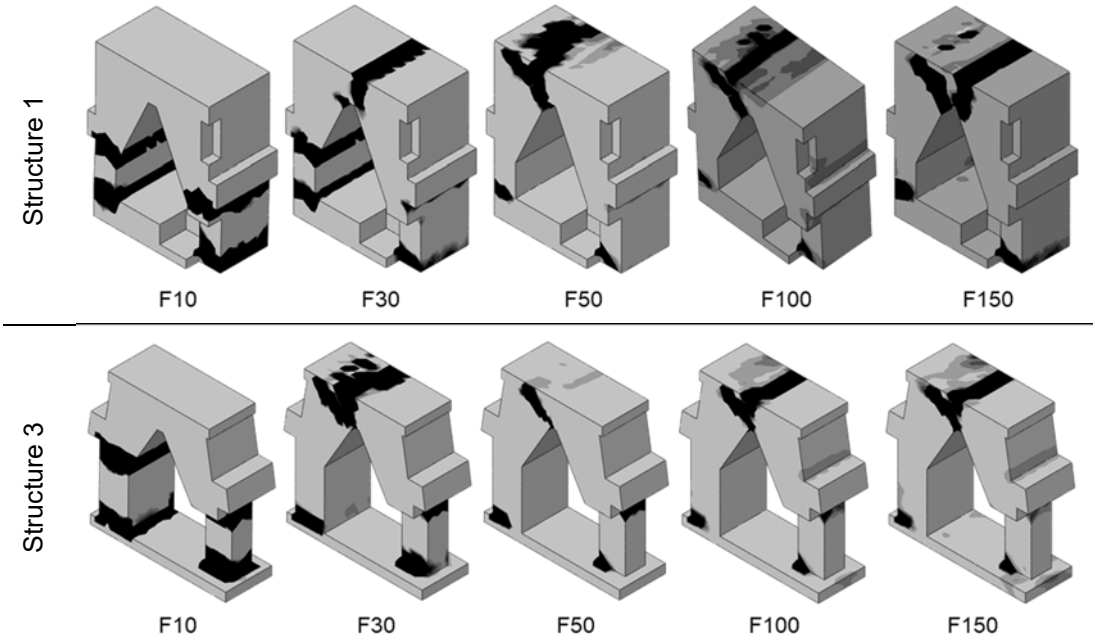

Figure 10 Sections for Structure 1 and Structure 3 (inclined) at failure instant for each tensile strength.

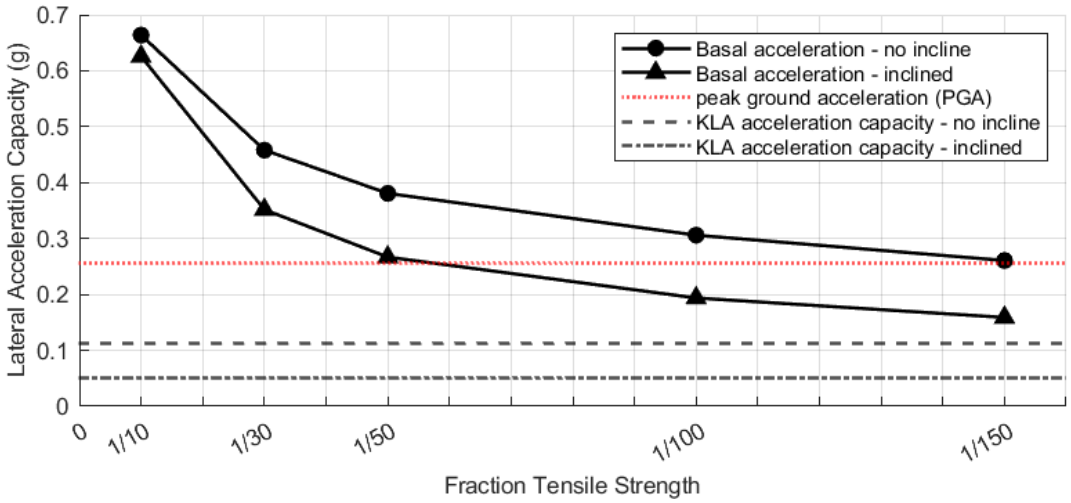

Figure 11 Structure 3 sections produce lateral capacity values that converge to the capacity determined from kinematic limit analysis as tensile strength decreases.

Because fracture patterns are dependent on the strength of the material, KLA models may not capture them correctly. The fracture patterns of the presented FE models show their dependence on material strength (

Figure 10).

4 Conclusions

This study proves for the present case that KLA substantially underestimates the lateral capacity of the structure. Therefore, it is of limited applicability in determining the necessary level of conservative intervention for this historical structure. This is because, by definition, KLA cannot include material strength. Our results show that material tensile strength fundamentally changes the analysis of monuments' lateral capacity and thus its seismic vulnerability. For Maya concrete, even a tensile strength value of F100, which is ten times smaller than the generally accepted 1/10 rule for tensile strength of masonry, generates a higher lateral capacity than KLA.

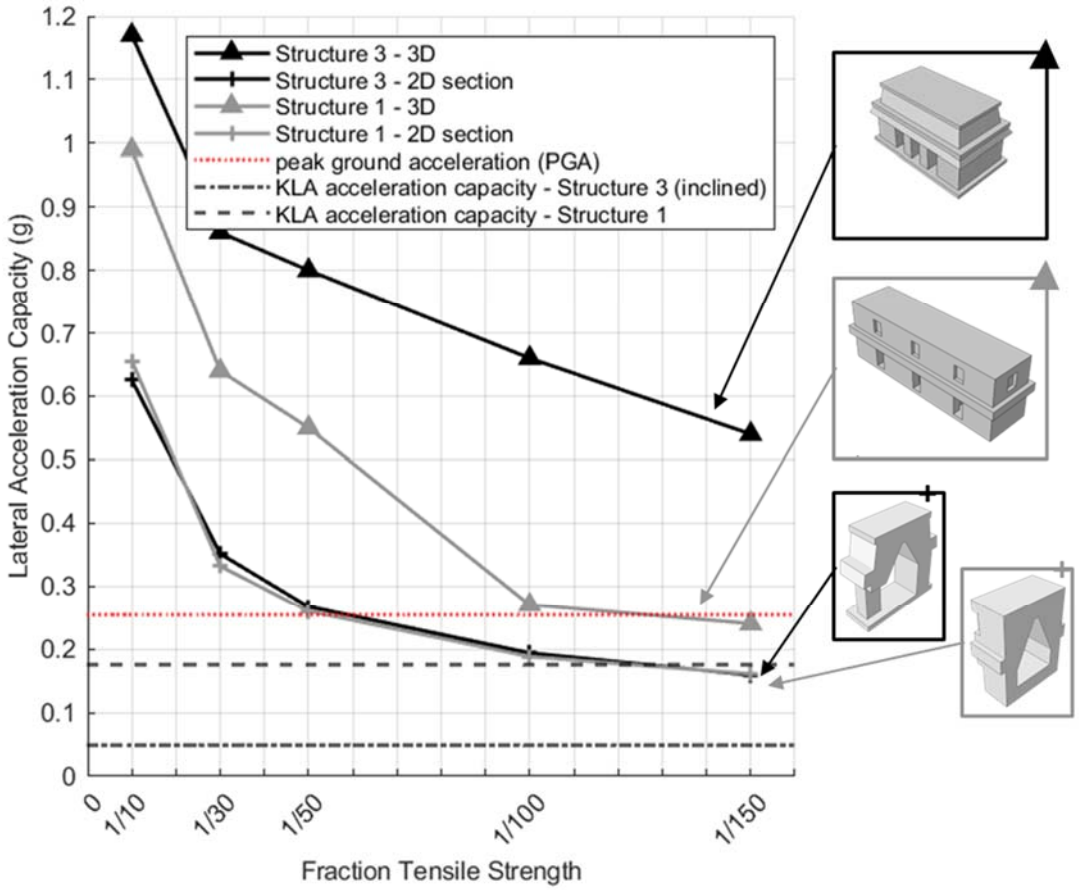

Figure 12 Comparison of 2D sectional and 3D models of Structure 1 and inclined Structure 3 (present state) with Chiapas peak ground acceleration (PGA) demand.

The cost of performing analysis that does not consider any material strength may result in overly invasive interventions that could disrupt the architectural appearance of the monument in the name of preservation. By omitting material strength from analyses, KLA may severely underestimate the ability of structures to sustain loads.

As shown in Figure 12, 2D sections of both structures produce similar results. Though their scale is slightly different (Structure 3 is smaller than Structure 1), the models' structural elements are similar: two columns supporting an arch. The present results suggest a strong connection between lateral capacity and missing structural elements, including shear walls and the span between them, that are captured by 3D models. Preliminary work in 3D supports this hypothesis [5,9]. The lateral capacities of 3D models retain structural integrity up to much higher levels of lateral acceleration, the result of including both the material effect of tensile strength and the additional structural effect of shear walls.

References

[1] Rodríguez-Lomelí AG, García-Mayordomo J. Seismic hazard at a triple plate junction: the state of Chiapas (México). Nat Hazards 2019;97:1297–325. https://doi.org/10.1007/s11069-019-03710-4.
[2] Ruppert K, Thompson JES, Proskouriakoff T. Bonampak, Chiapas, Mexico. Washington, D.C.: William Byrd Press; 1955.
[3] Structure 3. West end. n.d. https://doi.org/10.2307/artstor.11858868.
[4] Flores Espino C, Orea Magaña H. Vulnerability analysis of two Mayan vaulted structures aided by a genetic algorithm tool. In: Van Balen K, Verstrynge E, editors. Structural Analysis of Historical Constructions: Anamnesis, Diagnosis, Therapy, Controls. 4.3, CRC Press; 2016, p. 978–85. https://doi.org/10.1201/9781315616995-132.
[5] Hamad O, Sennyondo J, Kimanya H, Nguyen D, Tezcan S, Perucchio R. Structural Assessment Under Lateral Accelerations Of A Concrete Vaulted Maya Building Of Bonampak, Chiapas, Mexico 2022.
[6] Abaqus CAE/Explicit 2022.
[7] Roys L. The engineering knowledge of the Maya. Carnegie Institute of Washington 1934.
[8] Lubliner J, Oliver J, Oller S, Oñate E. A plastic-damage model for concrete. International Journal of Solids and Structures 1989;25:299–326. https://doi.org/10.1016/0020-7683(89)90050-4.
[9] Kimanya H, Remus A, Hamad O, Sennyondo J, Nguyen D, Tezcan S, et al. Seismic vulnerability assessment of vaulted Maya concrete temples in Bonampak, Chiapas, México. 9th ECCOMAS Thematic Conference on Computational Methods in Structural Dynamics and Earthquake Engineering, Athens, Greece: 2023.
[10] Angelillo M, Lourenço PB, Milani G. Masonry behaviour and modelling. In: Angelillo M, editor. Mechanics of Masonry Structures, vol. 551, Vienna: Springer Vienna; 2014, p. 1–26. https://doi.org/10.1007/978-3-7091-1774-3_1.